Human Replication Protein A Melts a DNA Triple Helix Structure in a Potent and Specific Manner†

Yuliang Wu‡, **Nina Rawtani‡**, **Arun Kalliat Thazhathveetil‡,§**, **Mark K. Kenny∥**, **Michael M. Seidman‡**, and **Robert M. Brosh Jr.*,‡**

Laboratory of Molecular Gerontology, National Institute on Aging, National Institutes of Health, 5600 Nathan Shock Drive, Baltimore, Maryland 21224, and Department of Emergency Medicine, Albert Einstein College of Medicine, Montefiore Medical Center, 111 East 210th Street, Bronx, New York 10467

Abstract

Alternate DNA structures other than double-stranded B-form DNA can potentially impede cellular processes such as transcription and replication. The DNA triplex helix and G4 tetraplex structures that form by Hoogsteen hydrogen bonding are two examples of alternate DNA structures that can be a source of genomic instability. In this study, we have examined the ability of human replication protein A (RPA), a single-stranded DNA binding protein that is implicated in all facets of DNA metabolism, to destabilize DNA triplexes and tetraplexes. Biochemical studies demonstrate that RPA efficiently melts an intermolecular DNA triple helix consisting of a pyrimidine motif third strand annealed to a 4 kb duplex DNA fragment at protein concentrations equimolar to the triplex substrate. Heterologous single-stranded DNA binding proteins (*Escherichia coli* SSB, T4 gene 32) melt the triplex substrate very poorly or not at all, suggesting that the triplex destabilizing effect of RPA is specific. In contrast to the robust activity on DNA triplexes, RPA does not melt intermolecular G4 tetraplex structures. Cellular assays demonstrated increased triplex DNA content when RPA is transiently repressed, suggesting that RPA melting of triple helical structures is physiologically important. On the basis of our results, we suggest that the abundance of RPA known to exist *in vivo* is likely to be a strong deterrent to the stability of triplexes that can potentially form from human genomic DNA sequences.

Alternate DNA structures that deviate from B-form double-stranded DNA such as bent, Z-form, triplex, and tetraplex DNA formations can be formed by sequences that are widely distributed throughout the human genome (for review, see refs 1-4). These secondary DNA structures are likely to have important effects on the stability of the genome and basic DNA metabolic processes. DNA triple helix and tetraplex structures are characterized by noncanonical Hoogsteen hydrogen bonding. Under physiological conditions, guanine-rich sequences can form four-stranded structures stabilized by planar arrays of guanines and the presence of a monovalent cation in the central cavity (5), (6). Triplexes are generated when a third strand lies in the major groove of duplex DNA and can occur most readily on polypurine–polypyrimidine sequences (7). The third strand may be composed of either pyrimidines or

SUPPORTING INFORMATION AVAILABLE

One figure showing SDS–PAGE and gel-shift analysis of single-stranded DNA binding proteins. This material is available free of charge via the Internet at http://pubs.acs.org.

purines, and the stability of the resulting triplex structure is dictated by the specific sequence. Triplexes form when an appropriate sequence partially melts with one of the single strands folding back to complex with an adjacent duplex. Triplexes have been shown to exist in chromosomes and nuclei (8), (9).

Growing evidence suggests that triplexes and tetraplexes are also likely to exist *in vivo* (10), (11). In support of this perspective, cellular proteins have been identified which bind to these alternate DNA structures (for review see refs 1,2, and 12), and certain helicases can unwind triplexes (13-15) and tetraplexes (16-20). It has been proposed that tetraplex structures play a role in telomere metabolism (for review see ref 11), immunoglobulin class switch recombination (11), (21), (22), nucleotide expansion disorders (2), and the expression of genes such as *c-myc* (23). Naturally occurring (H-DNA) triplex-forming sequences are also found in *c-myc* (24), (25). Naturally occurring triplexes are sources of genomic instability (26), and triplex-forming oligonucleotides can induce recombination or DNA repair (10). A number of inherited and acquired human diseases are associated with genomic instability of human DNA sequences that can form triplexes (1). For example, the triplex-forming potential of a $(GAA)_n$ repeat is proposed to lead to genomic instability and reduced frataxin gene expression, resulting in Friedreich's ataxia, a triplet repeat disorder (27). Triplex formation by the Friedreich's ataxia $(GAA)_n$ repeat inhibits DNA replication based on observations that the repeated sequence inhibits DNA polymerization *in vitro* (27), (28) and replication forks stall at $(GAA)_n$ repeats *in vivo* (29). Understanding the pathological basis for triplex-associated diseases and the mechanisms whereby cells prevent the deleterious effects of alternate DNA structures is clinically relevant. Moreover, the ability to form triplexes using oligonucleotides directed against specific target sequences has prompted their consideration as gene-targeting reagents (30-32). However, triplex formation *in vivo* may be at least partly inhibited by triplex-destabilizing proteins or helicases that exist in cells (13-15).

The single-stranded DNA binding protein RPA[1] has important roles in replication, recombination, DNA repair, and DNA damage signaling (for review see refs 33-35). RPA binds with high affinity to ssDNA and lower affinity to dsDNA and has also been reported to recognize and bind certain types of DNA damage. Although RPA has been implicated in specific cellular pathways, very little is known about its role in the metabolism of alternate DNA structures. Recently, the ability of RPA to destabilize an intramolecular G4 tetraplex structure formed by a human telomeric repeat sequence was described (36). RPA also directly binds triplex structures (37) and acts together with the DNA repair proteins XPA and XPC-hHR23B (37), (38) or high mobility group box (HMGB) 1 (39) to recognize triplex-induced helical distortions. In this study, we examined the ability of purified endogenous human RPA to melt DNA triplexes and tetraplexes and found that RPA destabilizes a DNA triple helix structure in a specific and highly effective manner.

EXPERIMENTAL PROCEDURES

Oligonucleotides

Oligonucleotides used for the preparation of triplex and tetraplex DNA substrates were purchased from Loftstrand Laboratories and are listed in Table 1.

Triplex DNA Substrate Preparations

The plasmid psupF5 contains a duplex sequence that serves as a target for TC30. Cleavage of the plasmid with *Nde*I released fragments of 4 and 0.6 kilobase pairs. The triplex site lies 1800

[1]Abbreviations: ESSB, *Escherichia coli* single-stranded DNA binding protein; gp32, gene 32 protein; RPA, replication protein A; XPA, xeroderma pigmentosum group A.

bases from one end of the large fragment. Triplexes were prepared by incubation of 3 pmol of 5′-^{32}P-labeled TC30 oligonucleotide (Table 1) (based on the molecular weights of the reaction components) overnight at room temperature with 6 pmol of *Nde*I-cleaved plasmid in a buffer containing 33 mM Tris–acetate (pH 5.5), 66 mM KOAc, 100 mM NaCl, 10 mM MgCl$_2$, and 0.1 mM spermine. The complexes were then separated from unbound oligonucleotide by gel filtration chromatography using Bio-Gel A-5 M resin. Restriction protection of the *Xba*I site which resides in the triplex target site was performed and demonstrated for the restriction fragment based triplex substrate as previously described (13).

The flush triplex substrates which contain triplex regions without underlying duplex extensions on either side of the triplex site consisted of either a 30 bp or 60 bp duplex annealed to a 30-mer third strand or 60-mer third strand, respectively. The 30-mer flush triplex substrates were prepared by incubation of the TC30 or 5MeC-TC30 oligonucleotide with the previously annealed 30 bp duplex (TC30W and TC30C) under the annealing conditions described above. Similarly, the 60-mer flush triplex substrates were prepared by incubation of the TC60 or 5MeC-TC60 oligonucleotide with the previously annealed 60 bp duplex (TC60W and TC60C) under the annealing conditions described above. T_m determinations of the TC30 or 5MeC-TC30 30-mer flush triplex substrates were performed as previously described (13).

The intramolecular triplex substrate was prepared by incubation of the radiolabeled TC100-foldback oligonucleotide under the annealing conditions described above.

Tetraplex DNA Substrate Preparation

Intermolecular G4 DNA substrates derived from human telomeric sequence 5′TeR2 (Table 1) or mouse immunoglobulin switch region sequence TP (Table 1) were prepared as described in refs 16 and 18, respectively.

Proteins

Human RPA containing all three subunits (RPA70, RPA32, RPA14) was purified from HeLa cells as previously described (40). *Escherichia coli* single-stranded DNA binding protein (ESSB) and T4 gene 32 protein (gp32) were purchased from Promega and Boehringer Mannheim, respectively. The purity of the RPA, ESSB, and gp32 proteins was evaluated by the detected migration of the proteins after SDS–PAGE on Coomassie-stained gels according to their predicted sizes (Supporting Information Figure 1A). DNA binding activity was evaluated by the ability of each protein to stably bind a radiolabeled 60-mer oligonucleotide as detected by gel mobility shift assay (Supporting Information Figure 1B). The DNA binding activities and gel-shift patterns by RPA, ESSB, and gp32 were similar to those previously reported (41-43).

Triplex and Tetraplex Destabilization Assays

Reaction mixtures (20 μL) contained 40 mM Tris-HCl (pH 7.4), 25 mM KCl (unless indicated otherwise), 5 mM MgCl$_2$, 2 mM dithiothreitol, 2% glycerol, 100 ng/μL bovine serum albumin, 10 fmol of the specified triplex or tetraplex DNA substrate (0.5 nM DNA substrate concentration), and the indicated RPA concentrations. Reactions were initiated by the addition of RPA and then incubated at 30 °C for 15 min or the specified temperature and time. For triplex reactions, a 10 μL aliquot of loading buffer (40% glycerol, 0.9% SDS, 0.1% bromphenol blue, 0.1% xylene cyanol) was added to the mixture at the end of incubation, and products were resolved on nondenaturing polyacrylamide gels (10% or 12% acrylamide as indicated in the figure legend, 40 mM Tris–acetate, pH 5.5, 5 mM MgCl$_2$, 25% glycerol) at 4 °C. For tetraplex reactions, a 20 μL aliquot of loading buffer (74% glycerol, 0.01% xylene cyanol, 0.01% bromphenol blue, 10 mM KCl, 20 mM EDTA) was added to the mixture at the end of incubation, and the products were incubated with proteinase K for an additional 15 min at 30

°C and subsequently resolved on nondenaturing 8% polyacrylamide gels. For gel-shift analysis to measure RPA binding to TP and 5′TeR2 tetraplex substrates, reaction conditions were the same as described above except proteinase K was omitted. Reaction products were resolved on nondenaturing 8% polyacrylamide gels. Radiolabeled DNA species on polyacrylamide gels were visualized with a PhosphorImager and quantitated using ImageQuant software (Amersham Biosciences).

ssDNA Electrophoretic Mobility Shift Assays

The indicated concentrations of RPA, ESSB, or gp32 were incubated with ^{32}P-labeled 60-mer oligonucleotide (TC60) (0.5 nM) in binding buffer containing 10 mM Tris-HCl (pH 7.4), 50 mM KCl, 0.5 mM DTT, and 10% glycerol at 25 °C for 15 min. After incubation, 3 μL of loading dye (74% glycerol, 0.01% xylene cyanol, 0.01% bromphenol blue) was added to each mixture, and samples were loaded onto native 5% (19:1 acrylamide:bisacrylamide) polyacrylamide gels and electrophoresed at 200 V for 2 h at 4 °C using 1× TBE as the running buffer.

RPA Silencing in HeLa Cells

RPA70 siRNA 1 was 5′-AACACUCUAUCCUCUUUCAUG-3′ (44). RPA70 siRNA 2 was 5′-AACUGGUUGACGAAAGUGGUG-3′ (45). The control siRNA was 5′-AGUUACUCAGCCAAGAACGA-3′. siRNA transfections were done using Lipofectamine 2000 (Invitrogen) according to manufacturer's protocol. HeLa cells were plated to 40% confluence in six-well plates 24 h prior to transfection. siRNA (100 pmol) (combined RPA70 siRNA 1 and 2) was mixed with 5 μL of Lipofectamine 2000 in 2.5 mL Opti-Mem (Invitrogen). The mixture was added to cells which were subsequently incubated for 6 h. After 24 h, a second transfection was performed similarly. Seventy-two hours after the initial transfection, cell lysates were collected for Western blot assay, or cells were fixed for immunofluorescence staining.

Immunofluorescence Staining

Cells were treated with siRNA as described above. Cells were washed twice with PBS and fixed with paraformaldehyde (3.7%) at room temperature for 15 min. Fixed cells were washed four times with PBS and treated with 0.5% Triton solution (Sigma) at room temperature for 3 min. Cells were then washed four times with PBS and blocked with 10% goat serum (Sigma) overnight at 4 °C. Indirect immunostaining was performed by first incubating cells with a triplex-specific mouse monoclonal antibody Jel 466 (8), (46) overnight at 4 °C. Following four washes in PBS with 0.1% Tween- 20, cells were incubated with Alexa Fluor 488 goat anti-mouse IgG (1:400, Invitrogen) for 1 h at 37 °C. Cells were washed four times with PBS containing 0.1% Tween-20 and coated with Prolong Gold antifade reagent containing DAPI (Invitrogen). Coverslips were placed on chamber slides, and cells were cured at room temperature in the dark for 24 h. Immunofluorescence was performed on a Zeiss LSM 510 META inverted Axiovert 200 M laser scan microscope with a Plan-Apochromat 63×/1.4 oil DIC objective. Images were captured with a CCD camera and analyzed using a LSM Browser software package.

RESULTS

RPA Melts a DNA Triplex Substrate

Increasing concentrations of RPA (0−24 nM heterotrimer) were incubated at 30 °C for 15 min with a DNA triplex substrate that consisted of a pyrimidine motif third strand (TC30) annealed to a 4 kb duplex restriction fragment that is stable at physiological pH. Products were resolved on native polyacrylamide gels. As shown in Figure 1A, melting of the triplex was dependent

on RPA concentration. Melting was detectable at RPA concentrations as low as 0.4 nM heterotrimer and achieved a plateau of 90% triplex melted at 6 nM RPA (Figure 1C).

To assess if RPA can melt a more stable DNA substrate, a triplex substrate with a pyrimidine motif third strand containing 5MeC throughout the sequence was tested since it is more stable at physiological pH. In the buffer used for the triplex destabilization assays, the T_m of the triple helix with 5MeC-TC30 was 57.9 °C, as previously reported (13), compared to 54.0 °C for the nonmethylated TC30 triplex substrate. As shown in Figure 1B, melting of the 5MeC-TC30 triplex substrate was dependent on RPA concentration. At a given RPA concentration, less 5MeC triplex was melted compared to the unmodified triplex; however, ~90% of the 5MeC triplex was destabilized at the highest RPA concentration tested, 24 nM (Figure 1C).

To characterize the requirements for the triplex melting activity of RPA, we examined the salt and temperature dependence of the reaction. At 37 °C, RPA destabilized 80% of the triplex substrate at physiological KCl concentrations (120−145 mM); however, less triplex was destabilized by RPA at the higher salt concentrations tested (Figure 2A,B). Some triplex destabilization by RPA was detected at higher salt concentrations (195, 245 mM) (Figure 2A,B). Triplex melting by RPA increased as a function of temperature from 20 to 40 °C (Figure 2C,D). At 145 mM KCl and 37 °C, triplex destabilization by RPA was dependent on time (Figure 2E,F). A total of 18% of the triplex substrate was melted by 1 min, and this percentage increased throughout the time course, achieving ~70% triplex melted at 16 min. In summary, these results indicate that RPA can destabilize triplex DNA under physiological conditions in a time-dependent manner.

Melting of DNA Triplexes by RPA Is Specific

We next asked if the ability of RPA to melt the triplex DNA substrate was specific or if heterologous single-stranded DNA binding proteins like ESSB or gp32 protein were able to melt the triplex substrate. As shown in Figure 3, neither ESSB nor gp32 could effectively melt the triplex, indicating that the triplex melting activity of RPA is specific and not a general property of single-stranded DNA binding proteins.

The Presence of ssDNA Can Compete for RPA To Melt the DNA Triplex

To characterize the ability of RPA to melt a triplex substrate, we asked if the presence of ssDNA with RPA (6 nM) and the triple helix substrate (0.5 nM) had an effect. Increasing concentrations of unlabeled ssDNA (X12−2) did inhibit RPA melting of the triple helix substrate; however, substantial inhibition of RPA triplex melting required 50-mer ssDNA concentrations of 6.2 nM and greater (Figure 4). At lower concentrations of 50-mer ssDNA (1.6, 3.2 nM), less inhibition (≤ 10%) was observed. The known high-affinity ssDNA binding site for RPA is 30 nt (34), suggesting that equimolar concentration of RPA ssDNA binding sites (one high-affinity site per 50-mer) compared to RPA binding equivalents can effectively compete for RPA to melt the DNA triplex substrate.

RPA Melts a DNA Triplex Substrate Lacking Duplex Extension

To assess the DNA structural elements important for RPA melting of triplex DNA, we examined its ability to melt a flush DNA triplex composed of a pyrimidine-rich third strand annealed to an oligonucleotide-based 30 bp duplex. Unlike the previous triplex substrate characterized by a 30-mer third strand annealed to a 4 kb duplex fragment, no underlying duplex extensions exist in the flush triplex substrate. For the flush 30-mer triplex substrate, the triplex site consisted of a 30 bp duplex annealed to a 30-mer third strand.

As shown in Figure 5, RPA was able to melt the flush 30-mer triplex substrate in a protein concentration-dependent manner. However, the melting of the flush triplex by RPA was not

nearly as efficient as the melting of the triplex substrate with an extended duplex (Figure 1). For example, at an RPA concentration of 3 nM, 80% of the triplex substrate that contained a duplex extension was melted (Figure 1A,C) whereas only 20% of the flush triplex was melted (Figure 5A,C). The difference was even greater at an RPA concentration of 1.5 nM in which 70% of the triplex substrate with an extended duplex was melted (Figure 1C) whereas only 10% of the flush triplex was melted (Figure 5C). We also noted that, for the flush triplex substrate, 12% of the underlying duplex was melted by 12 nM RPA (our unpublished data), whereas ~90% of the triplex was destabilized (Figure 5). Thus, significantly greater percentages of the triplex were melted than the underlying duplex at these RPA concentrations, consistent with our observations that the triplex is destabilized first followed by the duplex portion of the substrate (data not shown).

These results suggest that, for efficient RPA melting of triplex DNA, an extended underlying duplex is necessary. Although RPA melting of the flush triplex was not very efficient, RPA performed significantly better than ESSB, which only achieved ~20% melting of the flush triplex at the highest ESSB concentration tested, 24 nM (Figure 5C).

We also assessed the ability of RPA to melt the more stable flush triplex with a 5MeC third strand. As shown in Figure 5B, melting of the flush 30-mer 5MeC triplex substrate was dependent on RPA concentration. Although the 5MeC triplex was melted somewhat less efficiently by RPA compared to the unmodified triplex, ~90% of the 5MeC flush triplex was destabilized at the highest RPA concentration tested, 24 nM (Figure 5C). In comparison, ESSB acted very poorly to destabilize the 5MeC triplex (Figure 5C).

To determine if length of the flush triplex is a factor in the reduced efficiency of melting by RPA, experiments were performed with a flush triplex consisting of a 60-mer triplex-forming strand annealed to a 60 bp duplex. This substrate is twice as long as the 30-mer triplex used in the previous experiments. Quantitative analyses demonstrated that both the unmodified and 5MeC-modified 60-mer flush triplexes were melted with similar efficiency by RPA (Figure 6). Both the 30-mer and 60-mer flush triplexes were melted less efficiently by RPA compared to the triplex with TC30 embedded in an underlying (4 kb) duplex, suggesting that the low efficiency of RPA melting the 30-mer flush triplex is not likely due to substrate length.

RPA Can Melt an Intramolecular Triplex Structure

The ability of RPA to melt intermolecular triplex-forming oligonucleotide-generated triplexes raised the question if RPA might also be able to destabilize an intramolecular H-DNA triplex substrate that represents a more physiological structure that would form naturally. To address this, we tested RPA on an intramolecular triplex substrate derived from a single-stranded DNA molecule. The intramolecular triplex that forms contains a foldback duplex region that harbors an *Ear*I restriction site protected from *Ear*I cleavage by the annealed third strand. Incubation of RPA with the triplex substrate followed by *Ear*I digestion and analysis by gel electrophoresis demonstrated that RPA melts the intramolecular triplex in an RPA concentration-dependent manner (Figure 7).

RPA Fails To Melt Intermolecular G4 Tetraplex DNA Structures

The ability of RPA to efficiently melt a triplex DNA substrate raised the possibility that RPA might also melt other types of alternate DNA structures. The G4 DNA structure stabilized by noncanonical Hoogsteen hydrogen bonds between four G-rich strands is one such structure. We tested RPA for melting a well-characterized G4 structure derived from a mouse immunoglobulin sequence and found that RPA concentrations as high as 96 nM heterotrimer completely failed to melt the G4 structure which was at a concentration of 0.5 nM (Figure 8A). Under these conditions, RPA was able to effectively bind the G4 substrate as shown in Figure

8B. We also tested the effect of RPA on an intermolecular tetraplex structure derived from a human telomeric sequence and found that it failed to melt this structure under conditions in which the G4 structure was effectively bound by RPA (Figure 8C,D). At the higher RPA concentrations, multiple shifted bands were observed on the native gels for RPA binding to the TP-G4 and 5′TeR2-G4 substrates. Both of these substrates are four-stranded molecules with 5′ ssDNA tails of 21 and 15 nt, respectively. Hence, the multiple species detected at higher RPA concentrations are due to more than one RPA molecule binding to a single G4 substrate. At low concentrations of RPA (e.g., 1.5 nM), the higher mobility band is absent because multiple RPA molecules are not bound to each DNA substrate molecule. These results suggest that RPA poorly melts intermolecular G4 structures under conditions in which RPA efficiently melts DNA triplexes.

Increased Triplex DNA in RPA-Depleted Human Cells

To address if RPA is important in triplex DNA metabolism *in vivo*, we transiently repressed RPA70 expression by RNA interference and visualized nuclear triplex DNA by immunofluorescence using the triplex-specific antibody Jel 466 (8), (46). Two siRNA-RPA70 oligonucleotides reduced RPA70 protein level by greater than 90% as detected by Western blot analyses of HeLa cell extracts (Figure 9A). HeLa cells that were transfected with either a control siRNA or a combination of siRNA-RPA70 oligonucleotides 1 and 2 were immunologically stained for triplex DNA. The typical results from these experiments showed significantly greater (4-fold) immunostaining for triplex DNA in RPA70-depleted cells compared to the control cells (Figure 9B), suggesting that the ability of RPA to melt DNA triplex structures is biologically important.

DISCUSSION

There has been considerable interest in the roles of single-stranded DNA binding proteins to recognize specific types of DNA structures in a cascade of events to facilitate subsequent steps in DNA processing pathways. A key eukaryotic protein in virtually all aspects of cellular DNA metabolism is RPA (34); therefore, we examined the interaction of human RPA with alternate DNA structures which are proposed to interfere with basic cellular processes of DNA replication, recombination, and transcription and be a source of genomic instability. From this study, we report that RPA can melt a DNA triplex substrate enabling the third strand that resides in the major groove of the underlying duplex to be released. RPA destabilization of the triplex DNA structure occurs in an efficient and specific manner that is not merely dependent on ssDNA binding since heterologous single-stranded DNA binding proteins performed poorly in the triplex destabilization reaction. RPA was also able to melt more thermally stable 5MeC-TC30 triplexes, suggesting that the action of RPA is robust and specific since ESSB acted poorly to destabilize these triplex substrates. On a per mole basis, the triplex destabilizing activity of RPA on the 5MeC-TC30/4 kb triplex was significantly greater than the ATP-dependent unwinding activity of the Werner syndrome helicase (WRN) on a very similar triplex DNA substrate (13). Thus, RPA destabilizes a DNA triple helix structure in a manner that is specific and relatively effective.

In an earlier study, it was reported that RPA and the xeroderma pigmentosum group A protein (XPA) bind specifically and with high affinity to psoralen-cross-linked triplex DNA lesions (37). It was suggested by Vasquez et al. that RPA and XPA function together as a complex to recognize the structural distortion of a DNA triple helix and distinguish the alternate DNA structure from undamaged DNA, a critical early step of DNA damage recognition that signals nucleotide excision repair. In that study (37), DNA binding gel-shift experiments were performed with a covalent psoralen monoadducted triplex substrate; consequently, concentration-dependent binding of RPA to the covalent psoralen-cross-linked triplex was

observed, but RPA destabilization of the triplex substrate would not be recognized. In our studies with a non-cross-linked triplex substrate, RPA destabilization of the triplex was detectable at RPA concentrations that were equimolar with the triplex DNA substrate concentration. The robust triplex displacement by relatively low concentrations of RPA suggests that RPA efficiently recognized the flush 30 nt triple helix structure which was embedded within the 4 kb duplex fragment. This result is further supported by the ssDNA competition experiments in which we observed that ssDNA 50-mer concentrations less than the RPA heterotrimer concentration of 6 nM only had a minor effect of inhibiting triplex destabilization by RPA. Thus our results suggest that RPA recognizes, binds, and destabilizes a triple helix that is flanked by long duplex regions on either side of the triplex in a relatively efficient manner.

Although RPA was reported to unfold an intramolecular antiparallel G4 structure composed of four GGG blocks and derived from a 21-mer human telomeric repeat sequence (36), we did not detect any RPA melting of the intermolecular tetraplex structures presented by a human telomeric sequence containing two GGG blocks or a mouse immunoglobulin switch region sequence containing two GGGG blocks. This finding is potentially important since guanine tetraplex topology is likely to be determined by the number of (TTAGGG) repeats, as recently demonstrated for human telomere DNA (47). Our results suggest that the effect of RPA on tetraplex DNA may be dependent on its precise molecular structure. The finding that intermolecular antiparallel G4 DNA may promote telomere–telomere interactions and chromosome joining (48) suggests that the inability of RPA to destabilize intermolecular telomeric tetraplex structures is likely to be important in terms of genomic stability. The specificity of RPA for tetraplex dissociation may also be relevant to the proposal that intermolecular G4 structures may contribute to sister chromatid exchanges in BS cells (18).

The ability of RPA to melt alternate DNA structures is relevant to the roles of RPA in various cellular DNA metabolic processes in which ssDNA can transiently form and interact with other strands to form secondary and tertiary structures. Our results from cellular assays showing increased triplex DNA content when RPA is transiently repressed suggest that RPA melting of triple helical structures is physiologically important. Given that sequences with triplex-forming potential are widely distributed in the human genome (7), (27), (49-51), it is probable that if triplexes are not resolved, they will interfere with processes such as DNA replication or recombination. Triplexes were shown to arrest progression of Holliday junctions in a model system (52). Triplexes, like arrested replication forks, may be susceptible to breakage, consistent with the highly recombinogenic nature of triplex-forming sequences in human cells (53). Therefore, demonstration that RPA efficiently melts a DNA triple helix structure points to a broader role of RPA in cellular DNA metabolism that is likely to be physiologically important. It will be of interest to determine if or how the role of RPA in the destabilization of alternate DNA structures is regulated. For example, RPA phosphorylation is known to affect its physical and functional properties (33), (35), (54), which in turn may influence its ability to destabilize intermolecular or intramolecular alternate DNA structures associated with human diseases.

ACKNOWLEDGMENT

REFERENCES

1. Bissler JJ. Triplex DNA and human disease. Front. Biosci 2007;12:4536–4546. [PubMed: 17485395]

2. Fry M. Tetraplex DNA and its interacting proteins. Front. Biosci 2007;12:4336–4351. [PubMed: 17485378]

3. Phan AT, Mergny JL. Human telomeric DNA: G-quadruplex, i-motif and Watson-Crick double helix. Nucleic Acids Res 2002;30:4618–4625. [PubMed: 12409451]

4. Rich A, Zhang S. Timeline: Z-DNA: the long road to biological function. Nat. ReV. Genet 2003;4:566–572. [PubMed: 12838348]

5. Gellert M, Lipsett MN, Davies DR. Helix formation by guanylic acid. Proc. Natl. Acad. Sci. U.S.A 1962;48:2018. [PubMed: 13976054]2013

6. Gilbert DE, Feigon J. Multistranded DNA structures. Curr. Opin. Struct. Biol 1999;9:305–314. [PubMed: 10361092]

7. Manor H, Rao BS, Martin RG. Abundance and degree of dispersion of genomic d(GA)n · d(TC)n sequences. J. Mol. EVol 1988;27:96–101. [PubMed: 3137357]

8. Agazie YM, Burkholder GD, Lee JS. Triplex DNA in the nucleus: direct binding of triplex-specific antibodies and their effect on transcription, replication and cell growth. Biochem. J 1996;316(Part 2):461–466. [PubMed: 8687388]

9. Lee JS, Burkholder GD, Latimer LJ, Haug BL, Braun RP. A monoclonal antibody to triplex DNA binds to eucaryotic chromosomes. Nucleic Acids Res 1987;15:1047–1061. [PubMed: 2434928]

10. Chin JY, Schleifman EB, Glazer PM. Repair and recombination induced by triple helix DNA. Front. Biosci 2007;12:4288–4297. [PubMed: 17485375]

11. Maizels N. Dynamic roles for G4 DNA in the biology of eukaryotic cells. Nat. Struct. Mol. Biol 2006;13:1055–1059. [PubMed: 17146462]

12. Doherty KM, Sharma S, Gupta R Jr. Tetraplex Binding Molecules as Anti-Cancer Agents. Recent Pat. Anti-Cancer Drug DiscoVery 2006;1:185–200.

13. Brosh RM Jr. Majumdar A, Desai S, Hickson ID, Bohr VA, Seidman MM. Unwinding of a DNA triple helix by the Werner and Bloom syndrome helicase. J. Biol. Chem 2001;276:3024–3030. [PubMed: 11110789]

14. Kopel V, Pozner A, Baran N, Manor H. Unwinding of the third strand of a DNA triple helix, a novel activity of the SV40 large T-antigen helicase. Nucleic Acids Res 1996;24:330–335. [PubMed: 8628658]

15. Maine IP, Kodadek T. Efficient unwinding of triplex DNA by a DNA helicase. Biochem. Biophys. Res. Commun 1994;204:1119–1124. [PubMed: 7980585]

16. Fry M, Loeb LA. Human Werner syndrome DNA helicase unwinds tetrahelical structures of the fragile X syndrome repeat sequence $d(CGG)_n$. J. Biol. Chem 1999;274:12797–12802. [PubMed: 10212265]

17. Mohaghegh P, Karow JK Jr. Bohr VA, Hickson ID. The Bloom's and Werner's syndrome proteins are DNA structure-specific helicases. Nucleic Acids Res 2001;29:2843–2849. [PubMed: 11433031]

18. Sun H, Karow JK, Hickson ID, Maizels N. The Bloom's syndrome helicase unwinds G4 DNA. J. Biol. Chem 1998;273:27587–27592. [PubMed: 9765292]

19. Sun H, Bennett RJ, Maizels N. The *Saccharomyces cerevisiae* Sgs1 helicase efficiently unwinds G-G paired DNAs. Nucleic Acids Res 1999;27:1978–1984. [PubMed: 10198430]

20. Vaughn JP, Creacy SD, Routh ED, Joyner-Butt C, Jenkins GS, Pauli S, Nagamine Y, Akman SA. The DEXH protein product of the DHX36 gene is the major source of tetramolecular quadruplex G4-DNA resolving activity in heLa cell lysates. J. Biol. Chem 2005;280:38117–38120. [PubMed: 16150737]

21. Duquette ML, Pham P, Goodman MF, Maizels N. AID binds to transcription-induced structures in c-MYC that map to regions associated with translocation and hypermutation. Oncogene 2005;24:5791–5798. [PubMed: 15940261]

22. Larson ED, Duquette ML, Cummings WJ, Streiff RJ, Maizels N. MutSalpha binds to and promotes synapsis of transcriptionally activated immunoglobulin switch regions. Curr. Biol 2005;15:470–474. [PubMed: 15753043]

23. Siddiqui-Jain A, Grand CL, Bearss DJ, Hurley LH. Direct evidence for a G-quadruplex in a promoter region and its targeting with a small molecule to repress c-MYC transcription. Proc. Natl. Acad. Sci. U.S.A 2002;99:11593–11598. [PubMed: 12195017]

24. Kinniburgh AJ. A cis-acting transcription element of the c-myc gene can assume an H-DNA conformation. Nucleic Acids Res 1989;17:7771–7778. [PubMed: 2678005]

25. Mirkin SM, Lyamichev VI, Drushlyak KN, Dobrynin VN, Filippov SA, Frank-Kamenetskii MD. DNA H form requires a homopurine-homopyrimidine mirror repeat. Nature 1987;330:495–497. [PubMed: 2825028]

26. Wang G, Vasquez KM. Naturally occurring H-DNA-forming sequences are mutagenic in mammalian cells. Proc. Natl. Acad. Sci. U.S.A 2004;101:13448–13453. [PubMed: 15342911]

27. Gacy AM, Goellner GM, Spiro C, Chen X, Gupta G, Bradbury EM, Dyer RB, Mikesell MJ, Yao JZ, Johnson AJ, Richter A, Melancon SB, McMurray CT. GAA instability in Friedreich's Ataxia shares a common, DNA-directed and intraallelic mechanism with other trinucleotide diseases. Mol. Cell 1998;1:583–593. [PubMed: 9660942]

28. Ohshima K, Montermini L, Wells RD, Pandolfo M. Inhibitory effects of expanded GAA · TTC triplet repeats from intron I of the Friedreich ataxia gene on transcription and replication in vivo. J. Biol. Chem 1998;273:14588–14595. [PubMed: 9603975]

29. Krasilnikova MM, Mirkin SM. Replication stalling at Friedreich's ataxia (GAA)$_n$ repeats in vivo. Mol. Cell. Biol 2004;24:2286–2295. [PubMed: 14993268]

30. Kalish JM, Glazer PM. Targeted genome modification via triple helix formation. Ann. N.Y. Acad. Sci 2005;1058:151–161. [PubMed: 16394134]

31. Seidman MM. Oligonucleotide mediated gene targeting in mammalian cells. Curr. Pharm. Biotechnol 2004;5:421–430. [PubMed: 15544490]

32. Seidman MM, Puri N, Majumdar A, Cuenoud B, Miller PS, Alam R. The development of bioactive triple helix-forming oligonucleotides. Ann. N.Y. Acad. Sci 2005;1058:119–127. [PubMed: 16394131]

33. Fanning E, Klimovich V, Nager AR. A dynamic model for replication protein A (RPA) function in DNA processing pathways. Nucleic Acids Res 2006;34:4126–4137. [PubMed: 16935876]

34. Wold MS. Replication protein A: a heterotrimeric, single-stranded DNA-binding protein required for eukaryotic DNA metabolism. Annu. ReV. Biochem 1997;66:61–92. [PubMed: 9242902]

35. Zou Y, Liu Y, Wu X, Shell SM. Functions of human replication protein A (RPA): from DNA replication to DNA damage and stress responses. J. Cell. Physiol 2006;208:267–273. [PubMed: 16523492]

36. Salas TR, Petruseva I, Lavrik O, Bourdoncle A, Mergny JL, Favre A, Saintome C. Human replication protein A unfolds telomeric G-quadruplexes. Nucleic Acids Res 2006;34:4857–4865. [PubMed: 16973897]

37. Vasquez KM, Christensen J, Li L, Finch RA, Glazer PM. Human XPA and RPA DNA repair proteins participate in specific recognition of triplex-induced helical distortions. Proc. Natl. Acad. Sci. U.S.A 2002;99:5848–5853. [PubMed: 11972036]

38. Thoma BS, Wakasugi M, Christensen J, Reddy MC, Vasquez KM. Human XPC-hHR23B interacts with XPARPA in the recognition of triplex-directed psoralen DNA interstrand crosslinks. Nucleic Acids Res 2005;33:2993–3001. [PubMed: 15914671]

39. Reddy MC, Christensen J, Vasquez KM. Interplay between human high mobility group protein 1 and replication protein A on psoralen-cross-linked DNA. Biochemistry 2005;44:4188–4195. [PubMed: 15766246]

40. Kenny MK, Schlegel U, Furneaux H, Hurwitz J. The role of human single-stranded DNA binding protein and its individual subunits in simian virus 40 DNA replication. J. Biol. Chem 1990;265:7693–7700. [PubMed: 2159011]

41. Jones CE, Mueser TC, Nossal NG. Bacteriophage T4 32 protein is required for helicase-dependent leading strand synthesis when the helicase is loaded by the T4 59 helicase-loading protein. J. Biol. Chem 2004;279:12067–12075. [PubMed: 14729909]

42. Lee SH, Kim DK. The role of the 34-kDa subunit of human replication protein A in simian virus 40 DNA replication in vitro. J. Biol. Chem 1995;270:12801–12807. [PubMed: 7759535]

43. Lohman TM, Overman LB, Datta S. Salt-dependent changes in the DNA binding co-operativity of *Escherichia coli* single strand binding protein. J. Mol. Biol 1986;187:603–615. [PubMed: 3519979]

44. Zou L, Elledge SJ. Sensing DNA damage through ATRIP recognition of RPA-ssDNA complexes. Science 2003;300:1542–1548. [PubMed: 12791985]

45. Wu X, Shell SM, Zou Y. Interaction and colocalization of Rad9/Rad1/Hus1 checkpoint complex with Replication protein A in human cells. Oncogene 2005;24:4728–4735. [PubMed: 15897895]

46. Raghavan SC, Chastain P, Lee JS, Hegde BG, Houston S, Langen R, Hsieh CL, Haworth IS, Lieber MR. Evidence for a triplex DNA conformation at the bcl-2 major breakpoint region of the t(14;18) translocation. J. Biol. Chem 2005;280:22749–22760. [PubMed: 15840562]

47. Vorlickova M, Chladkova J, Kejnovska I, Fialova M, Kypr J. Guanine tetraplex topology of human telomere DNA is governed by the number of (TTAGGG) repeats. Nucleic Acids Res 2005;33:5851–5860. [PubMed: 16221978]

48. Schaffitzel C, Berger I, Postberg J, Hanes J, Lipps HJ, Pluckthun A. In vitro generated antibodies specific for telomeric guanine-quadruplex DNA react with Stylonychia lemnae macronuclei. Proc. Natl. Acad. Sci. U.S.A 2001;98:8572–8577. [PubMed: 11438689]

49. Bacolla A, Collins JR, Gold B, Chuzhanova N, Yi M, Stephens RM, Stefanov S, Olsh A, Jakupciak JP, Dean M, Lempicki RA, Cooper DN, Wells RD. Long homopurine*homopyrimidine sequences are characteristic of genes expressed in brain and the pseudoautosomal region. Nucleic Acids Res 2006;34:2663–2675. [PubMed: 16714445]

50. Brereton HM, Firgaira FA, Turner DR. Origins of polymorphism at a polypurine hypervariable locus. Nucleic Acids Res 1993;21:2563–2569. [PubMed: 8332453]

51. Gaddis SS, Wu Q, Thames HD, DiGiovanni J, Walborg EF, MacLeod MC, Vasquez KM. A web-based search engine for triplex-forming oligonucleotide target sequences. Oligonucleotides 2006;16:196–201. [PubMed: 16764543]

52. Benet A, Azorin F. The formation of triple-stranded DNA prevents spontaneous branch-migration. J. Mol. Biol 1999;294:851–857. [PubMed: 10588891]

53. Rooney SM, Moore PD. Antiparallel, intramolecular triplex DNA stimulates homologous recombination in human cells. Proc. Natl. Acad. Sci. U.S.A 1995;92:2141–2144. [PubMed: 7892237]

54. Binz SK, Sheehan AM, Wold MS. Replication protein A phosphorylation and the cellular response to DNA damage. DNA Repair (Amsterdam) 2004;3:1015–1024.
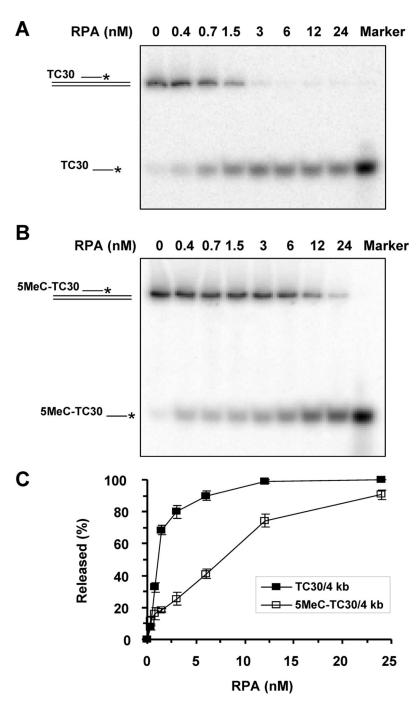
Figure 1.
RPA melts an intermolecular DNA triple helix. Panel A: The indicated concentration of RPA was incubated for 15 min at 30 °C with a triplex DNA substrate (0.5 nM) consisting of either TC30 (panel A) or 5MeC-TC30 (panel B) annealed to a triplex target site within a 4 kb restriction fragment as described in Experimental Procedures. Products were resolved on native 12% polyacylamide gels. The marker is radiolabeled TC30 oligonucleotide (panel A) or 5MeC-TC30 oligonucleotide (panel B). Quantitative analyses of the data are shown in panel C. Data represent the mean of at least three independent experiments with SD indicated by error bars.
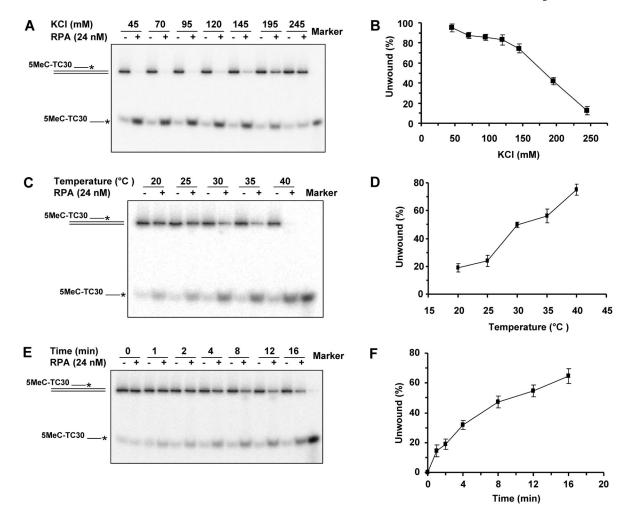
Figure 2.
Salt, temperature, and time dependence of RPA melting a DNA triple helix. Panel A: RPA (24 nM) was incubated with the indicated concentrations of KCl for 15 min at 37 °C with the 5MeC-TC30/4 kb triplex DNA substrate (0.5 nM) as described in Experimental Procedures. Panel C: The triplex DNA substrate 5MeC-TC30 (0.5 nM) was incubated for 15 min in reaction mixtures containing 145 mM KCl at the indicated temperature in the presence or absence of RPA (24 nM). Panel E: The triplex DNA substrate 5MeC-TC30 (0.5 nM) was incubated in reaction mixtures containing 145 mM KCl for the indicated times in the presence or absence of RPA (24 nM). Products were resolved on native 12% polyacylamide gels. The marker is radiolabeled 5MeC-TC30 oligonucleotide. Quantitative analyses of the data in panels A, C, and E are shown in panels B, D and F, respectively. Data represent the mean of at least three independent experiments with SD indicated by error bars.
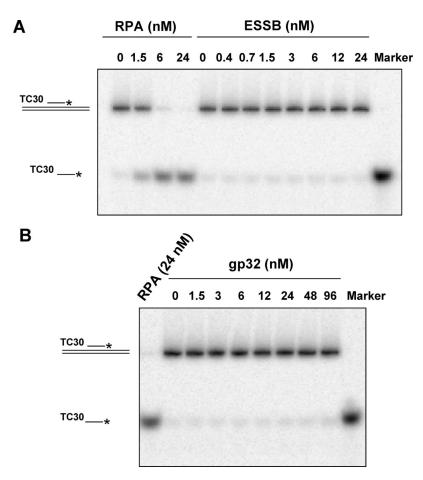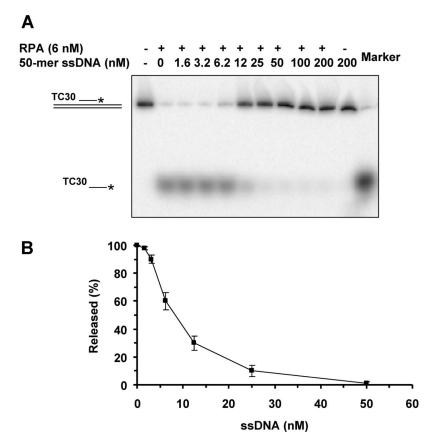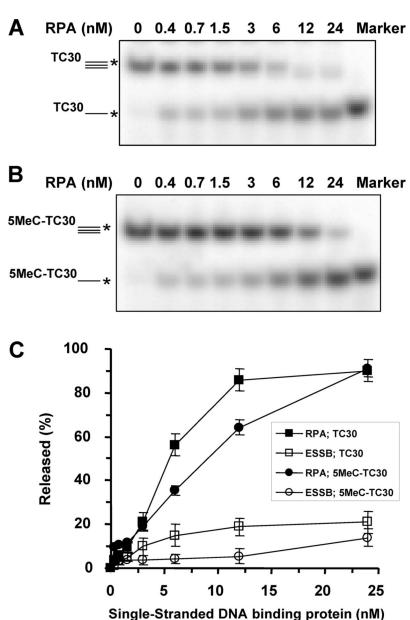
FIgure 3.
Neither *E. coli* SSB nor T4 gene 32 protein melts the triplex DNA substrate. The indicated concentration of ESSB (panel A) or gp32 (panel B) was incubated with the TC30:4 kb triplex DNA substrate (0.5 nM) for 15 min at 30 °C as described in Experimental Procedures. In control reactions, the indicated concentration of RPA was incubated with triplex DNA substrate under standard conditions. Products were resolved on native 12% polyacylamide gels. The marker is radiolabeled TC30 oligonucleotide. Representative gels from at least four independent experiments are shown.

A

RPA (6 nM)   -   +   +   +   +   +   +   +   +   +   -
50-mer ssDNA (nM)   -   0 1.6 3.2 6.2 12 25 50 100 200 200 **Marker**

TC30 ___*

TC30 ___*

B

Figure 4.
A molar excess of ssDNA inhibits RPA melting of the DNA triplex. Panel A: RPA (6 nM) was added to the reaction mixture containing the TC30:4 kb triplex substrate (0.5 nM) on ice for 1 min, and the indicated concentrations of unlabeled 50-mer oligonucleotide X12−2 (Table 1) were subsequently added. The reaction mixtures were immediately incubated at 30 °C for 15 min. Products were resolved on native 12% polyacylamide gels. The marker is radiolabeled TC30 oligonucleotide. Quantitative analyses of data are shown in panel B. Data represent the mean of at least three independent experiments with SD indicated by error bars.

Figure 5.
Activity of RPA or ESSB on a 30-mer flush DNA triplex with no duplex DNA extension. Panel A: The indicated concentration of RPA was incubated with 0.5 nM 30-mer flush triplex DNA substrate with annealed TC30 (panel A) or 5MeC-TC30 (panel B) for 15 min at 30 °C as described in Experimental Procedures. Products were resolved on native 10% polyacylamide gels. The marker is radiolabeled TC30 oligonucleotide (panel A) or 5MeC-TC30 oligonucleotide (panel B). Quantitative analyses of data from RPA (filled squares) and ESSB (open squares) experiments with TC30 flush triplex substrate or RPA (filled circles) and ESSB (open circles) with 5MeC-TC30 flush triplex substrate are shown in panel C. Data represent the mean of at least three independent experiments with SD indicated by error bars.
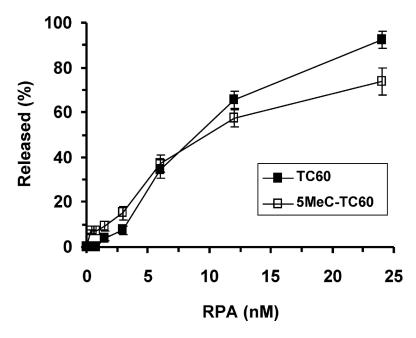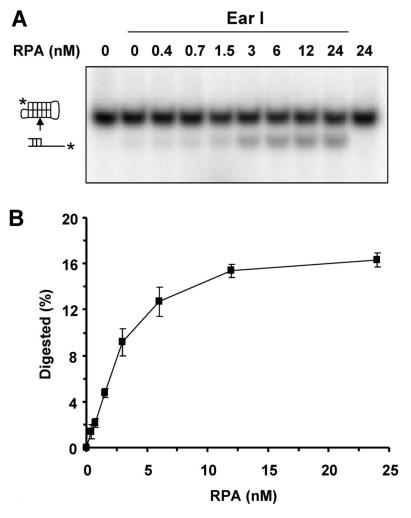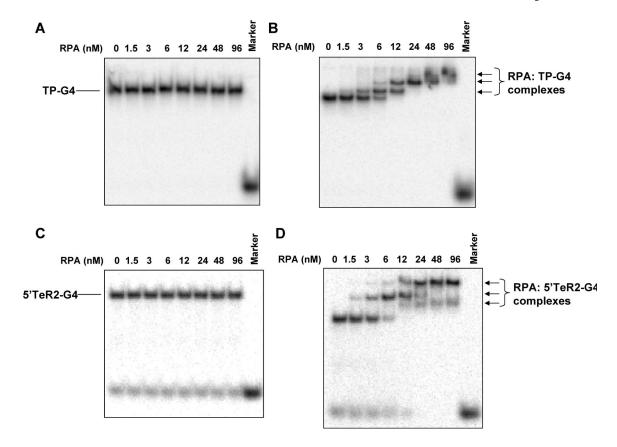
Figure 6.
Activity of RPA on a 60-mer flush DNA triplex. The indicated concentrations of RPA were incubated with 0.5 nM 60-mer flush triplex DNA substrate with annealed TC60 or 5MeC-TC60 for 15 min at 30 °C as described in Experimental Procedures. Products were resolved on native 10% polyacylamide gels. Quantitative analyses of data from RPA experiments with TC60 flush triplex substrate (filled squares) or 5MeC-TC60 flush triplex substrate (open squares) are shown. Data represent the mean of at least three independent experiments with SD indicated by error bars.

Figure 7.
RPA melts an intramolecular DNA triple helix. Panel A: The indicated concentration of RPA was incubated for 15 min at 30 °C with an intramolecular triplex DNA substrate (0.5 nM) derived from a TC100-foldback oligonucleotide as described in Experimental Procedures. After the RPA incubation, the reaction mixture was digested with *Ear*I restriction endonuclease (digestion site indicated by arrowhead), and products were resolved on native 10% polyacylamide gels. Triplex protection from *Ear*I digestion is shown by the absence of cleavage product when RPA was not incubated with the intramolecular triplex (second lane). Quantitative analyses of the data are shown in panel B. Data represent the mean of at least three independent experiments with SD indicated by error bars.

Figure 8.
RPA fails to melt G4 tetraplex DNA structures.The indicated concentration of RPA was incubated with 0.5 nM G4 tetraplex DNA substrate derived from a mouse immunoglobulin sequence (panels A and B) or human telomeric sequence (panels C and D) for 15 min at 30 °C as described in Experimental Procedures. Products were either treated with proteinase K (panels A and C) or left untreated (panels B and D) and resolved on native 8% polyacylamide gels. The marker is radiolabeled TP (panels A and B) or 5′TeR2 (panels C and D) oligonucleotide. Representative gels from at least four independent experiments are shown.
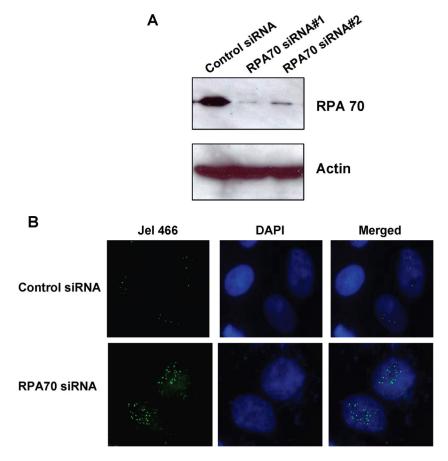
Figure 9.
Depletion of RPA70 increases intracellular triplex DNA content. Panel A: Small interfering RNA inhibition of RPA70. Whole cell extracts from HeLa cells that had been transfected with control or RPA70 siRNA (oligonucleotide 1 or 2) were subjected to Western blotting with RPA70 (catalog no. NA13, Calbiochem) or actin (catalog no. A2228, Sigma) antibodies (as a loading control). Panel B: Indirect immunofluorescence was performed on HeLa cells that had been transfected with either control siRNA or a combination of RPA70 siRNA oligonucleotides 1 and 2 as described in Experimental Procedures. Cells were coimmunostained with antitriplex Jel 466 antibody (green) and DAPI (blue).

Table 1

DNA Oligomers Used in This Study

oligomer	nucleotide sequence (5′–3′)
TC30[a]	TCTTTTTCTTTCTTTTCTTCTTTTTTCTTT
TC30W	TTTCTTTTTTCTTCTTTTTCTTTCTTTTTCT
TC30C	AGAAAAAGAAAGAAAGAAGAAAAAAGAAA
TC60[a]	TTTTCTTCTTTTTTTCTTTCTTTTTCTTCTC TTTTCTTTTTTCTTTTTCTT TTTTCTTTT
TC60W	TTTTCTTTTTTCTTTTTCTTTTTTCTTTT CTCTTCTTTTTCTTTCTTTTTTTCTTCTTTT
TC60C	AAAAGAAGAAAAAAAAGAAAGAAAAAAGAAG AGAAAAGAAAAAAGAAAAAGAAAAAA GAAAA
TC100-foldback[b]	TCTTTTTCTTTCTTTTCTTCTCTTTTCTTTTTT TTTTTCTTTTCTCTTCT↓TTTCTTTCTTTTTCTT TTTTAGAAAAAGAAAGAAAAGAAGAGAA AAGAAA
TP[c]	TGGACCAGACCTAGCAGCTAT<u>GGGGG</u>AG CT<u>GGGG</u>AA<u>GG</u>T<u>GGG</u>AATGTGA
5′TeR2[c]	TCATGACTAGACATGTTA<u>GGG</u>TTA<u>GGG</u>TTA
X12–2	CGGGTCAACGTGGGCAAAGATGTCCTAGCA ATGTAATCGTCTATGACGTC

[a]The cytosines in the 5MeC-TC30 and 5MeC-TC60 oligonucleotides are 5-methylcytosines with the same sequence as TC30 and TC60.

[b]Digested site of *Ear*I is marked by an arrow.

[c]The guanine residues that compose the G-quartet structures in oligonucleotides are underlined.